Hindawi
International Journal of Photoenergy
Volume 2018, Article ID 4549154, 12 pages
https://doi.org/10.1155/2018/4549154

Research Article

In Situ Low-Temperature Chemical Bath Deposition of CdS Thin Films without Thickness Limitation: Structural and Optical Properties

Mouad Ouafi,[1] **Boujemaâ Jaber**,[2] **Lahoucine Atourki**,[3,4] **Najwa Zayyoun**,[1] **Ahmed Ihlal**,[4] **Ahmed Mzerd**,[3] **and Larbi Laânab**[1]

[1]*LCS, Faculty of Science, Mohammed V University, Rabat, Morocco*
[2]*Materials Science Platform, UATRS Division, CNRST, Rabat, Morocco*
[3]*LPM, Faculty of Science, Mohammed V University, Rabat, Morocco*
[4]*LMER, Faculty of Science, Ibn Zohr University, Agadir, Morocco*

Correspondence should be addressed to Mouad Ouafi; mouad.ouafi@um5s.net.ma

Received 28 April 2018; Revised 16 July 2018; Accepted 29 July 2018; Published 27 August 2018

Academic Editor: Jinn Kong Sheu

In this work, thin CdS films have been deposited using the chemical bath deposition technique (CBD). Different synthesis parameters, such as number of runs, deposition time, and postannealing temperature, are studied and optimized in order to avoid the supersaturation phenomenon and to achieve a low-temperature growth. CdS thin films, of cubic structure, oriented along the (111) direction with homogenous and smooth surface, have been deposited by using the CBD growth process without any annealing treatment. Based on a set of experimental observations, we show that the solution saturation phenomenon can be avoided if the deposition is performed in several runs at a short deposition time. Throughout the CBD technique, it is then possible not only to overcome any film thickness limitation but also to grow the CdS films in a single technological step at a low temperature and without any postdeposition annealing treatment. CdS films with excellent structural quality and a controllable thickness are obtained when the deposition bath temperature is fixed at 65°C. In addition, deposited films exhibit an optical transmittance ranging from 70 to 95% depending on the synthesis parameters, with band gap energy around 2.42 eV. The process developed in this work might be useful for depositing CdS films on flexible substrates.

1. Introduction

Thin semiconductor films show a great potential for environmental and energy-related applications owing to their abundant unique characteristics [1–5]. Among these films, the CdS ones have drawn the attention of the research community due to their unique optoelectronic properties which include a large direct band gap (2.42 eV at room temperature), excellent optical and electronic properties, and a high chemical stability [6]. In addition, the CdS compound is one of the most suitable partners for heterojunction solar cells as a window layer when used in association with absorber layers like cadmium telluride (CdTe), copper indium gallium selenide/sulfide (CIGS), kesterites (CZTS) [7], or perovskites as an electron transport layer [8–10]. CdS also has potential applications in several fields, such as photocatalysis [11], laser [12, 13], light-emitting diodes, and field effect transistors [14].

CdS thin films can be synthesized using several deposition techniques through various physical and chemical methods such as molecular beam epitaxy (MBE) [15], sputtering [16], thermal evaporation [17], spray pyrolysis [18], chemical bath deposition [19], successive ionic layer adsorption and reaction [20], and electrodeposition [21]. Among these techniques, chemical bath deposition (CBD) is a simple and cheap method that can produce uniform and adherent large-area films [22]. Hereafter, this method was adopted to prepare the CdS thin films presented in this

study. According to previous works, the quality of CdS thin films prepared by the CBD technique depends strongly on various synthesis parameters such as the deposition time [23], the bath and annealing temperature [24, 25], the ammonia agent complex [26], and the concentrations of the chemical reagents [27],

Unfortunately, when seeking to synthesize CdS thin films by CBD, two major problems are generally encountered: (i) the postannealing treatment, which is a classical essential step for film crystallinity improvement, usually inducing a strong Cd thermal diffusion [28] and prevents the CdS deposition to be extended to flexible substrates [29], and (ii) the film thickness limitation, which is attributed to the solution supersaturation phenomenon [23, 30]. To overcome these problems, the synthesis process has been carried out in several runs. Based on experimental measurements, we show that the "number of runs" is a key parameter that affects strongly the structural, optical, and morphological properties of the synthesized CdS thin films. When compared to many reported works [23, 29–31], the obtained experimental results show that it is possible to achieve a desired film thickness only by controlling the number of cycles and/or the deposition time. Consequently, when these two parameters are optimized, the problem of supersaturation of the solution, observed in the literature [23, 30–33], can be avoided. Moreover and contrary to the reported works [24, 29, 30, 34], this technique allows growing in situ films, in a single technological step, at low temperature and without any postdeposition annealing treatment. Thus, the process developed in this work is considered as a relevant candidate when seeking to deposit CdS films on flexible substrates used in the embedded electronic systems.

2. Experimental Detail

CdS thin films used in this study are grown through heterogeneous reaction, on a glass substrate of 25 mm × 15 mm, by CBD technique. Two solutions named A and B have been firstly prepared separately. Solution A, considered as the cadmium source, is obtained by mixing 10^{-2} M of $CdCl_2$ and 3.6×10^{-2} M of NH_4Cl, while solution B, considered as the sulfur source, is the mixture of 1.7×10^{-2} of SC $(NH_2)_2$ and 3.6×10^{-2} M of NH_4Cl. Both mixtures were prepared in water solvent at room temperature. They are secondly individually heated at 45°C in a water bath until they become transparent, then mixed under continuous magnetic stirring (300–400 rpm) to obtain solution C. Before deposition, the glass substrates were ultrasonically cleaned in acetone and ethanol, rinsed in distilled water, dried in air, then vertically immersed into solution C with the help of Plexiglas holders. Our deposition method consists in stabilizing the temperature of the chemical bath (solution C) and substrate at an appropriate value (65°C ± 3°C) and then adding the ammonia drop by drop in order to maintain the pH at approximately 10. Right after, the solution color goes from transparent to orange indicating the start of CdS growth. After an appropriate deposition time, the first run is achieved. The successive runs were performed under the same conditions as the first one. It is worth noting that between two successive runs, the growing films do not undergo any thermal pyrolysis or postannealing treatment, but they are only submitted to an ultrasonic treatment to remove the poorly adhered CdS particles on their surface and then dried in air. The preparation conditions of annealed CdS thin films are presented in Table 1. After the preparation step, the film structure is determined by the PANalytical X'Pert Pro X-Ray Diffractometer, using CuKα (1.5406 Å) radiation source. Scanning electron microscopy coupled to EDS (Quanta 200) is used to observe the surface morphology and to perform the chemical composition analysis of the films. The optical transmittance is measured at room temperature using the Lambda 900 PerkinElmer spectrophotometer in the 300–1100 nm range.

Table 1: Conditions for preparing the CdS films.

Sample	Annealing temperature (°C)	Deposition time (min)	Number of runs
A	As-deposited	5	3
B	100	5	3
C	300	5	3
D	400	5	3
E	550	5	3

3. Results and Discussions

In the chemical bath deposition, the ammonia is a complexing agent which controls the release of metal (Cd^{2+}) and sulfur (S^{2-}) ions in the alkaline solution. The classical growth mechanism can be summarized by the following chemical reactions [35, 36]:

(1) The solution of amino-cadmium complex equilibrium:

$$Cd^{2+} + 4NH_3 \leftrightarrows Cd(NH_3)_4^{2+} \quad (1)$$

The formation of $Cd(NH_3)_4^{2+}$ prevents the precipitation of $Cd(OH)_2$.

(2) Hydrolysis of thiourea in an alkaline medium:

$$(NH_2)_2CS + OH^- \leftrightarrows SH^- + CH_2N_2 + H_2O \quad (2)$$

where SH^- ions are in equilibrium with water and give S^{2-} ions according to this equation:

$$SH^- + OH^- \leftrightarrows S^{2-} + H_2O \quad (3)$$

(3) Cadmium sulfide formation:

$$Cd(NH_3)_4^{2+} + S^{2-} \rightarrow CdS + 4NH_3 \quad (4)$$

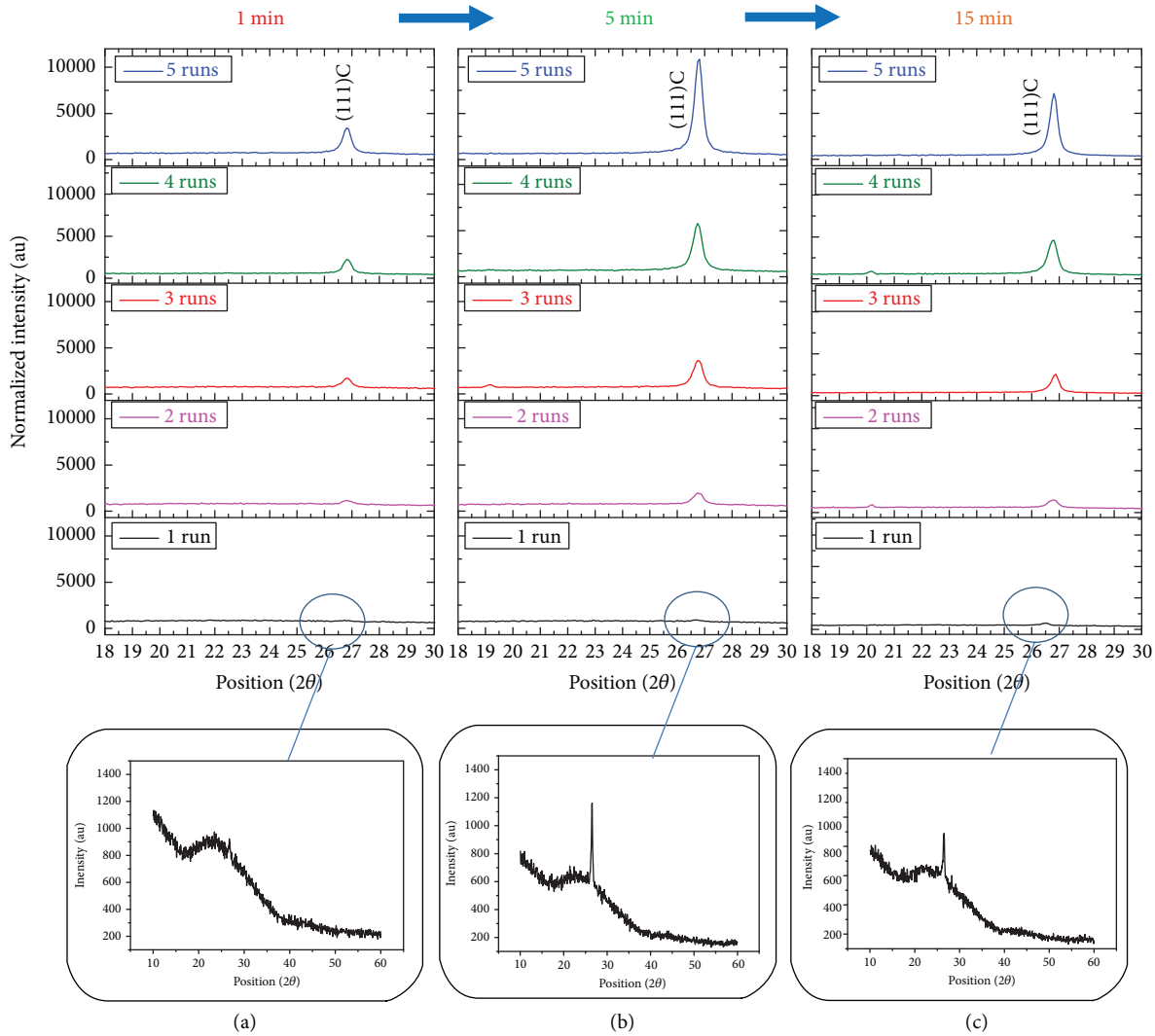

Figure 1: X-ray diffractograms of CdS thin films prepared in different runs and deposition times: (a) 1 min, (b) 5 min, and (c) 15 min.

The global reaction of CdS formation can be summarized as

$$\mathrm{Cd(NH_3)_4^{2+} + SC(NH_2)_2 + 2OH^- \xrightarrow{NH_4OH} CdS + CH_2N_2 + 4NH_3 + 2H_2O} \quad (5)$$

3.1. Structural Analysis. Figure 1 displays the XRD patterns of CdS thin films deposited in several runs (1–5 runs) at different deposition times (1–15 min). Each deposition is characterized by the number of runs and the deposition time of each run. Only the peak at 2θ equal to 26.81°, corresponding to the (111) plan of the CdS cubic structure, is observed for all the films. It is obvious that the intensity of the observed peak depends strongly on the number of runs and/or the deposition time. The highest intensity is recorded when the process is performed in 5 runs of 5 min. To do better, the variation of the crystalline quality as a function of these two parameters is examined by means of the crystalline ratio (R) defined by the following equation:

$$R = \frac{I(\text{run number, deposition time})}{I_{(1\text{ run},1\text{ min})}}, \quad (6)$$

where $I_{(\text{run number, deposition time})}$ is the (111) peak intensity at a given number of runs and deposition time and $I_{(1\text{ run},1\text{ min})}$ is the lowest (111) peak intensity obtained for the sample synthesized in a single run during one minute.

The variation of the crystalline ratio (R), deduced from Figure 1, as a function of the number of runs and deposition time is illustrated in Figure 2(a). It shows clearly that, regardless of the deposition time, all the CdS films deposited in only one run present low crystalline ratios indicating the poor crystallinity of the films. This behavior can be attributed to the amorphous structure of the glass substrate [37, 38]. However, the figure shows also that the (111) peak intensity of each sample increases speedily as the number of runs is

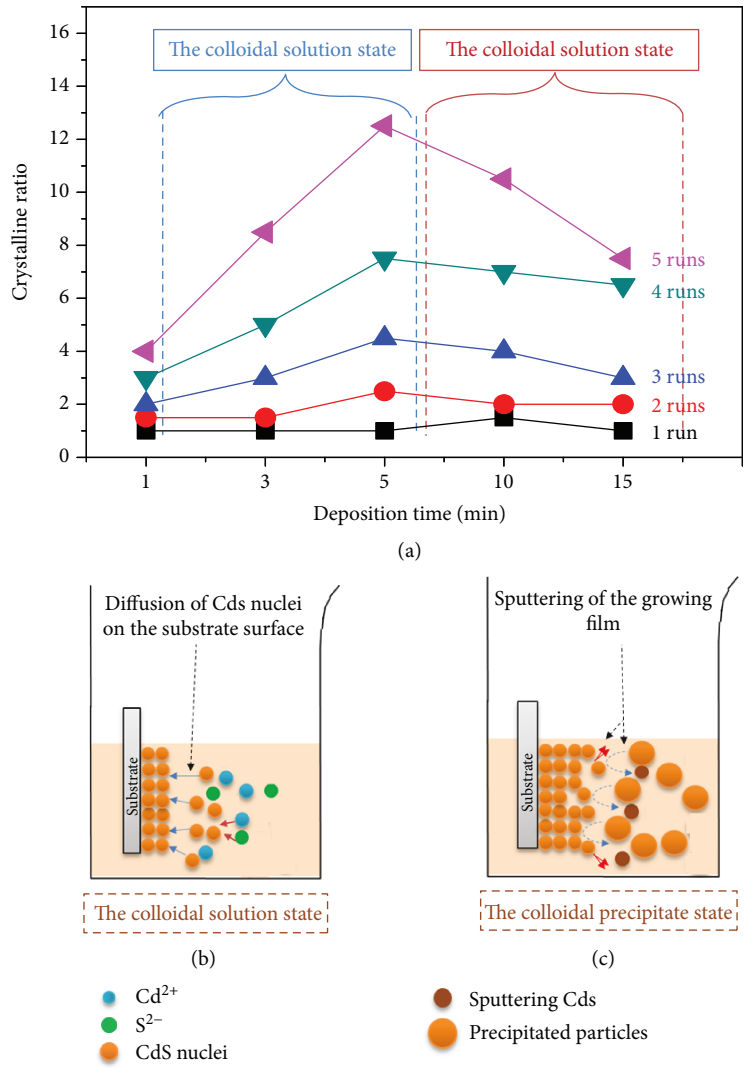

Figure 2: (a) Variation of the crystalline ratio as a function of number of runs and deposition time. Schematic representation of the growth states: (b) the colloidal solution state and (c) the colloidal precipitate state.

increased. The observed improvement of film crystallinity is attributed to (i) the increase in the material quantity as the number of runs is increased and/or (ii) the deposition is performed on a buffer layer which has already been crystallized. As far as the "deposition time" axis is concerned, two regions can be obviously distinguished in Figure 2(a): (i) a colloidal solution state region is observed when the deposition time is less than 5 min, in which the CdS thin films are formed throughout a nucleation growth mechanism [39]. In fact, just after the addition of ammonia, nuclei are firstly formed on the substrate surface, then grown by diffusion and finally closely adsorbed to form the film (see Figure 2(b)). In this region, an increase of the crystalline ratio is observed as the deposition time increases up to 5 min, which represents the optimal deposition time. This comportment has been also reported by many authors [23, 30]. (ii) A colloidal precipitate state region takes place when the deposition time exceeds 5 min. It is initiated by the appearance of the solution supersaturation phenomenon, where precipitated particles come to pulverize relatively the growing film (see Figure 2(c)), leading to the reduction of both the film thickness and the crystalline ratio as experimentally observed. A similar behavior has been observed by Tec-Yam et al. [40]. Based on these results, we can state that deposition in successive runs, with deposition time less or equal to 5 min, is preferred to avoid the solution supersaturation phenomenon. According to Figure 2(a), 5 min is considered as the optimal deposition time which allows the formation of CdS layers with the best crystallinity.

Figure 3(a) illustrates XRD patterns corresponding to the as-deposited (sample A) and annealed CdS thin films in air atmosphere (samples: B, C, D, and E) during 1 hour. A highly intense single peak at 26.55° is simultaneously observed for the as-deposited film and also for annealed ones at temperatures lower or equal to 400°C. In general, this atomic position can be attributed to the hexagonal or cubic structure of the CdS phase. However, compared to JCPDS card number 80-0019 and as suggested by Mahdi et al. [41], the absence of (100) and (101) peaks in the pattern (Figure 1(a)) confirms the formation of a (111)-oriented CdS cubic structure. As

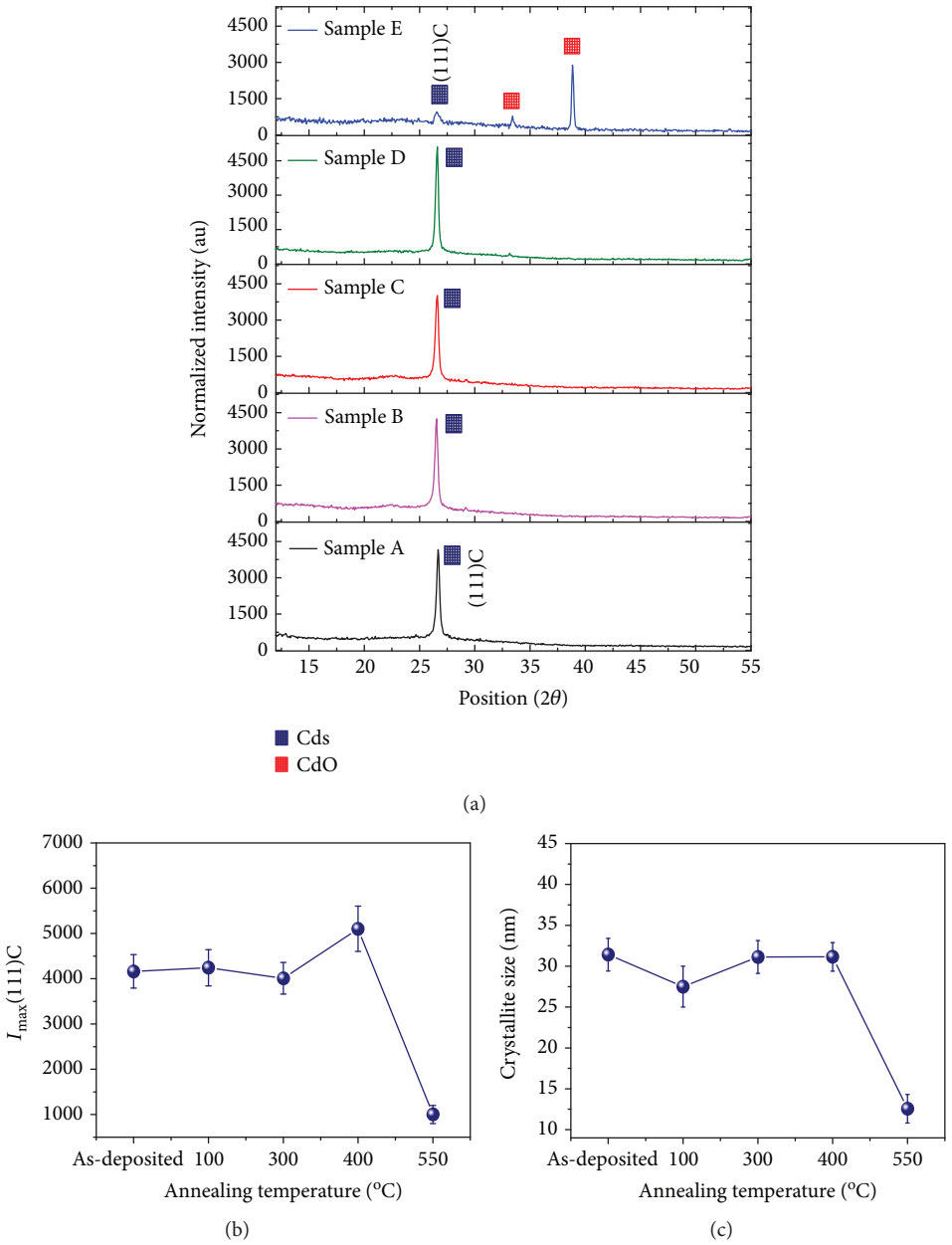

Figure 3: X-ray diffraction analysis of CdS thin films. (a) XRD spectra of the as-deposited and annealed CdS films. (b) Variation of the maximum intensity of the (111) peak as a function of the annealing temperature. (c) Variation of the grain size with the annealing temperature.

illustrated in Figure 3(b), only a slight increase of the (111) intensity is noticed when the temperature is increased up to 400°C. This suggests that the crystallization of the as-deposited film is achieved throughout the surface reaction kinetic of the Cd^{2+} and S^{2-} ions under the effect of bath temperature and substrate which is kept at 65°C. By contrast, the film annealed at temperature of 550°C shows a dramatic reduction of CdS (111) intensity and the appearance of other major peaks located at the positions of 32.83° and 38.07°. When compared to the JCPDS card number 78-0653, the two later peaks indicate the formation of CdO phases which are attributed to CdS oxidation. This oxidation took place because the annealing was performed in oxygen ambient [16]. Subsequently, we can state that the annealing treatment slightly improves the crystallinity when the temperature is below 400°C; nevertheless, it becomes destructive and leads to the formation of other phases when the temperature is above 400°C.

According to the XRD data of the CdS (111) plan, the crystallite size can be calculated by the following Scherrer formula:

$$D = \frac{0.94\lambda}{\beta \cos \theta}, \tag{7}$$

where λ (1.5406 Å) is the X-ray wavelength, θ is the Bragg angle, and β is the full width at half maximum (FWHM)

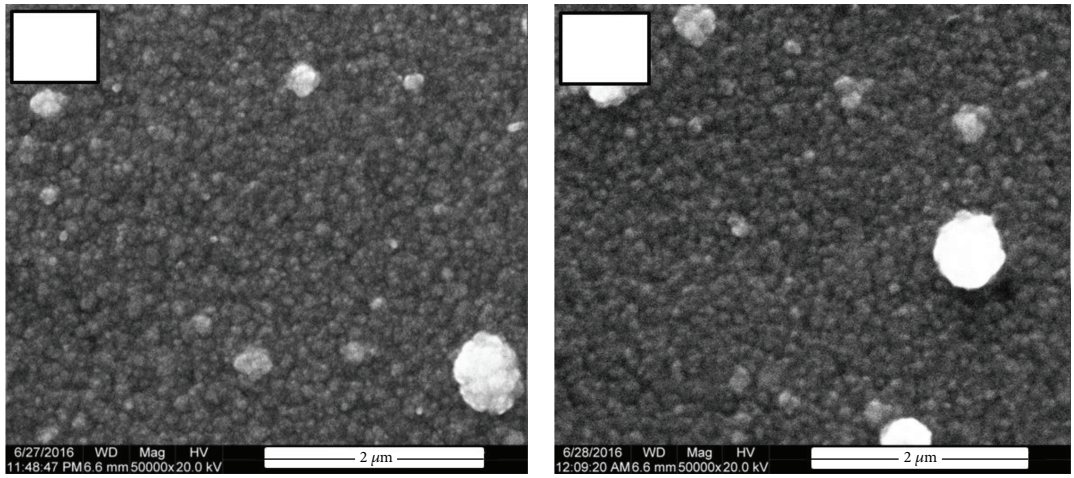

(a) (b)

Figure 4: SEM micrographs of CdS thin films: (a) as deposited (sample A) and (b) annealed at 400°C (sample D).

of the diffraction peak in radians. Figure 3(c) shows the variation of the CdS crystallite with the annealing temperature. No remarkable change in the mean crystallite size (about 30 nm) is observed when the annealing temperature is increased up to 400°C. Meanwhile, sample E, which is annealed at 550°C, exhibits a very small crystallite size indicating a drastic decomposition phenomenon of CdS into the CdO phase. These observations show clearly that our process permits to deposit CdS films with good crystallinity without any subsequent annealing treatment. Thus, it is then possible to manage CdS deposition at a lower temperature on substrates, even those which are instable at high temperatures, particularly the flexible ones.

3.2. Morphological Study. To investigate the effect of annealing on the morphological characteristics of CdS thin films, Figure 4 presents the surface SEM micrographs of samples A (Figure 4(a)) and D (Figure 4(b)). In both samples, homogeneous distributions of nanometric grains cover uniformly the surfaces. Grains are smooth and dense, and no evident morphological change is observed before and after the annealing treatment.

Figure 5 presents the SEM micrographs (a, b, and c) and the cross-sectional views of CdS thin films prepared at various numbers of runs (1, 3, and 5 runs). The obtained optimal deposition time of 5 min has been chosen. The micrographs show dense structures and smooth and relatively void-free surfaces. In each sample, the grains are well-defined, spherical, and homogeneously sized. It is worth noting that the increase in the number of runs has no significant effect on the grain sizes. Meanwhile, a few agglomerated particles are still observed on the surface; this fact is probably attributed to the slight saturated solution in the end of deposition time (for each run). Based on the cross sections SEM images, the film thickness values of 180, 320, and 580 nm have been measured for 1, 3, and 5 runs, respectively. These last values are very close to that obtained from transmittance spectra (Figure 6).

3.3. Energy-Dispersive Spectroscopy (EDS) Analysis. Results of EDS analysis performed on the CdS structure (spectrum "a") and agglomerated particle (spectrum "b") are presented in Figure 7. Table 2 reports the average chemical composition (weight and atomic percentage) of the two areas. It appears that both areas are constituted of Cd and S with some additional peaks of Si, O, Al, Na, and Mg which are attributed to the glass substrate chemical elements. It is clear that the average atomic percentage of S/Cd for both studied zones is in a near stoichiometric ratio of approximately 0.97.

3.4. Optical Characterizations

3.4.1. Thickness Film Calculation. Based on [42, 43], the thickness of the films (d) is calculated from the transmission interference fringes between 530 and 1100 nm using the following equation:

$$d = \frac{M\lambda_1\lambda_2}{2(\lambda_1 n_2 - \lambda_2 n_1)}, \tag{8}$$

where n_1 and n_2 are the refractive indices corresponding to two adjacent maxima (or minima) at wavelengths of λ_1 and λ_2, respectively.

$M = 1$ for two adjacent extremes of transmittance spectrum (max–max or min–min), and M = 1/2 for two adjacent unlike extremes (max–min or min–max) [44].

The refractive index (n) of the film over the transparent region can be calculated using [42, 43]

$$n = \left[N + \left(N^2 - s^2\right)^{1/2}\right]^{1/2}, \tag{9}$$

where s is the refractive index of the substrate (in our case, s = 1.51) and N is given by [45]

$$N = \frac{2s(T_{max} - T_{min})}{T_{max}T_{min}} + \frac{\left(s^2 + 1\right)}{2} \tag{10}$$

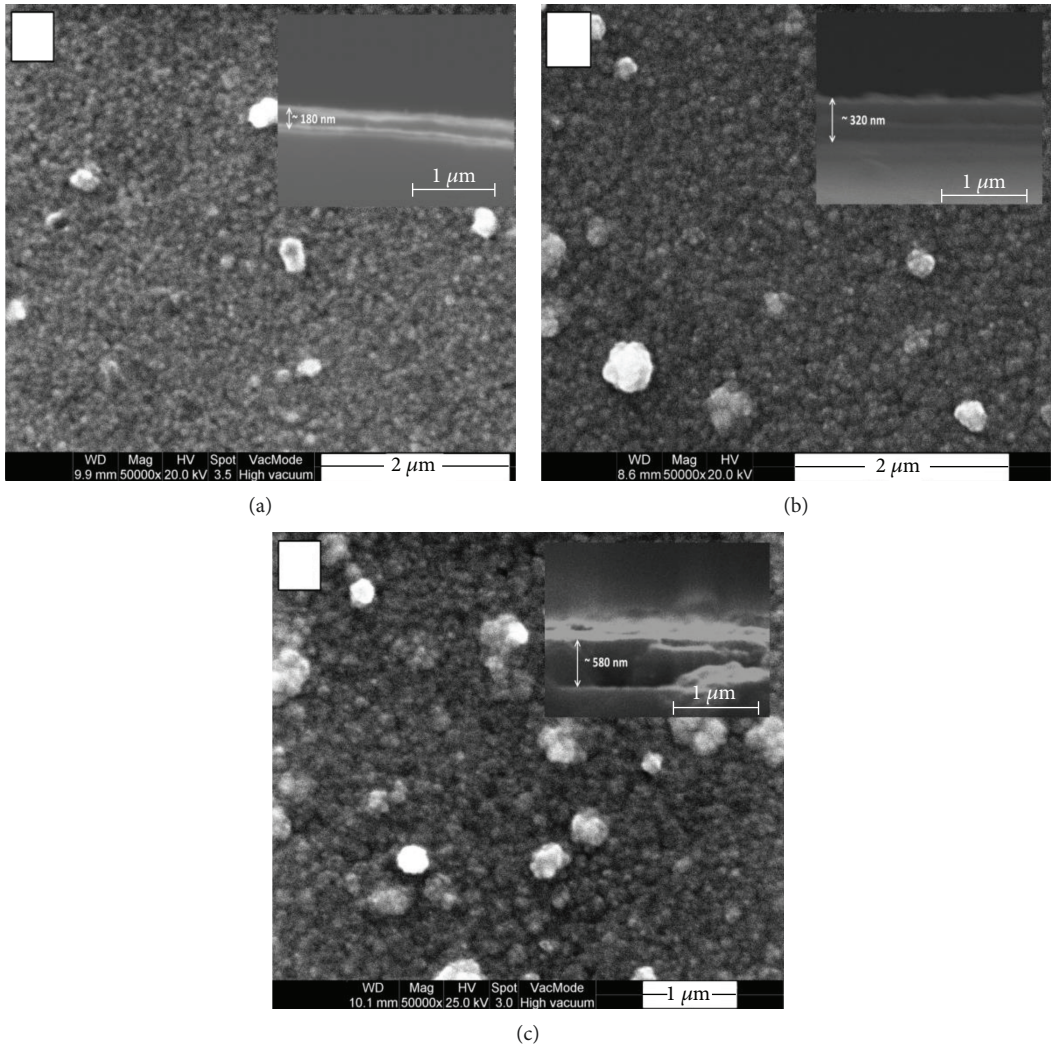

Figure 5: SEM micrographs and cross-sectional view of CdS thin films: (a) 1 run, (b) 3 runs, and (c) 5 runs with the deposition time of 5 min.

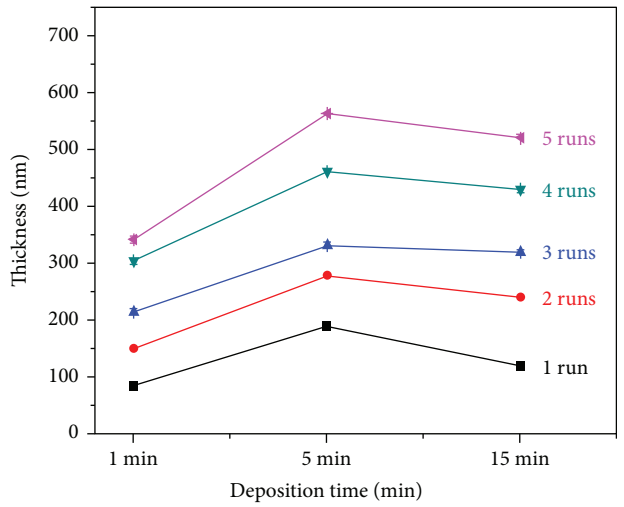

Figure 6: Variation of the film thickness as a function of the number of runs and deposition time.

where $T_{max}(\lambda)$ and $T_{min}(\lambda)$ are the transmission values at the maxima and minima of the interference fringes, and (s) is the refractive index of the glass substrate ($s = 1.51$). The refractive index values n_1 and n_2 of the CdS thin film (3 runs, 5 min) are found to be 2.11 and 2.06.

3.4.2. Transmittance, Thickness, Optical Band Gap, and Absorbance of CdS Thin Films. Figure 8 shows the optical transmittance spectra of CdS thin films in the wavelength range 300–2000 nm. The A, B, C, D, and E samples are highly transparent (~80%) in the visible and near-infrared regions of the electromagnetic spectrum and present a sharp cut-off at approximately 550 nm. Therefore, no additional improvement of the film transmittance is achieved by the annealing step. The measured average transmittances and thicknesses of the as-deposited film and the annealed ones are reported in Table 3. The high average transparency (~80%) and the appearing interference fringes in the visible and near-infrared regions of all CdS films (except for 550°C) attest that the light is less

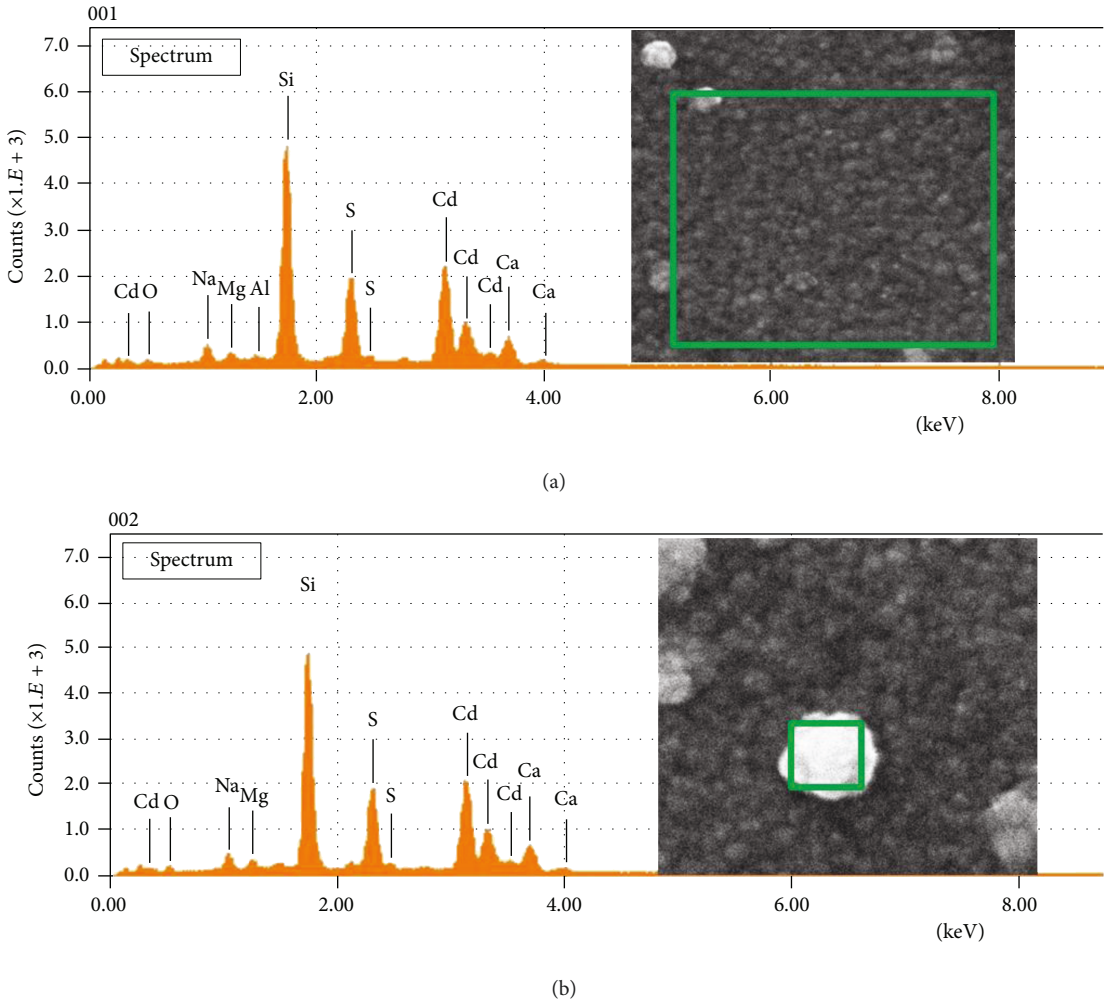

Figure 7: EDS analysis performed on the CdS structure (spectrum "a") and agglomerated particle (spectrum b).

Table 2: The compositional analyses of the CdS structure and agglomerated particles.

	Atomic %		Weight %	
	Cd	S	Cd	S
CdS structure	50.72	49.27	78.29	21.70
Agglomerated particles	50.59	49.40	78.22	21.77

scattered and the film surfaces are smooth and homogeneous with a very similar thickness of about 254 nm [44]. When the annealed temperature reaches 550°C, again drastic decreases of the optical transmittance (70%) and thickness (219 nm) are noticed. As revealed above by XRD analysis, the observed changes at high annealing temperature are attributed to the decomposition of the CdS film to the CdO phase.

The optical band gap (E_g) of CdS films was estimated by assuming a direct transition between valence and conduction

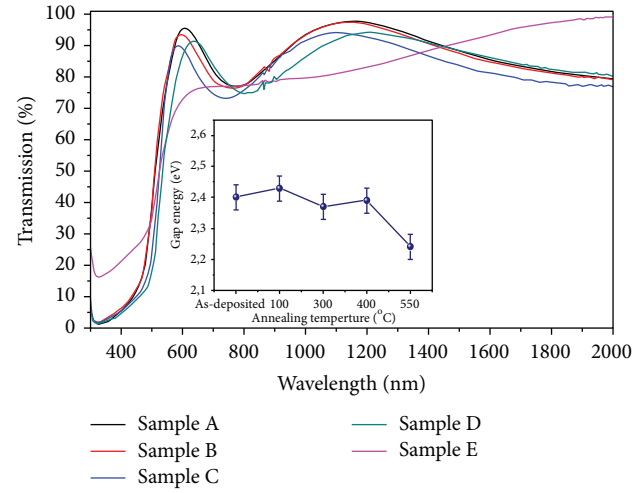

Figure 8: UV-Vis transmission spectra and the gap energy of as-deposited (sample A) and annealed CdS thin films (samples: B, C, D, and E).

Table 3: Thickness and average transmission values of the as-deposited (sample A) and annealed CdS thin films (samples B, C, D, and E).

Sample	Thickness (nm)	T_{ave} (%) (visible region)
A	254 ± 4	82
B	251 ± 4	81
C	253 ± 4	80
D	259 ± 4	79
E	219 ± 4	70

bands from the plot of $(\alpha h\nu)^2$ as a function of photon energy $h\nu$ according to the expression

$$(\alpha h\nu)^2 = A\left(h\nu - E_g\right), \tag{11}$$

where $h\nu$ is the photon energy, α is the absorption coefficient, and A is a constant. E_g is determined by extrapolating the linear portion of the spectrum to zero absorption coefficients. The intercept on the energy axis gives the value of the band gap energy. As it can be deduced from Figure 8, no significant change in the optical band gap value (around 2.41 eV) is observed between the as-deposited and annealed films (up to 400°C). However, the band gap energy of 2.24 eV obtained for the film annealed at 550°C matches well with the reported band gap value of CdO [46].

Figure 9 displays the transmission spectra, in wavelengths ranging from 300 to 1100 nm, of CdS thins films prepared at various numbers of runs and deposition times. When increasing the number of runs from 1 to 5, the average transmission at wavelength greater than 500 nm is increased from 55 to 91%, 80 to 94%, and 74 to 86% when the deposition times are 1 min (Figure 9(a)), 5 min (Figure 9(b)), and 15 min (Figure 9(c)), respectively. The highest optical transmittance (94%) is recorded when the deposition is performed in 4 runs of 5 min. By contrast, all CdS thin films deposited in whatever the deposition time (1, 5, or 15 min) exhibit a strong transmission tail in the 300–500 nm range, indicating that the films are thinner with a poor crystallinity [47]. However, when the number of runs is varied from 2 to 5, all spectra show a sharp fall at the band edge which is shifted towards the longer wavelengths as the number of runs increases. This observed shift is likely due to the increase in the film thickness as it has been reported by many authors [43, 44]. However, the perceived interference fringes attest to the film quality [44, 48] and help to estimate the thickness of CdS layer.

Figure 6 presents the variation of the film thickness as a function of the number of runs and the deposition time. It is clear that regardless the number of runs, (i) the film thickness increases as a function of deposition time up to 5 min, because at this deposition time range the film grows in the colloidal solution state. The estimated thickness films at 5 min are 190, 280, 332, 462, and 564 nm when the number

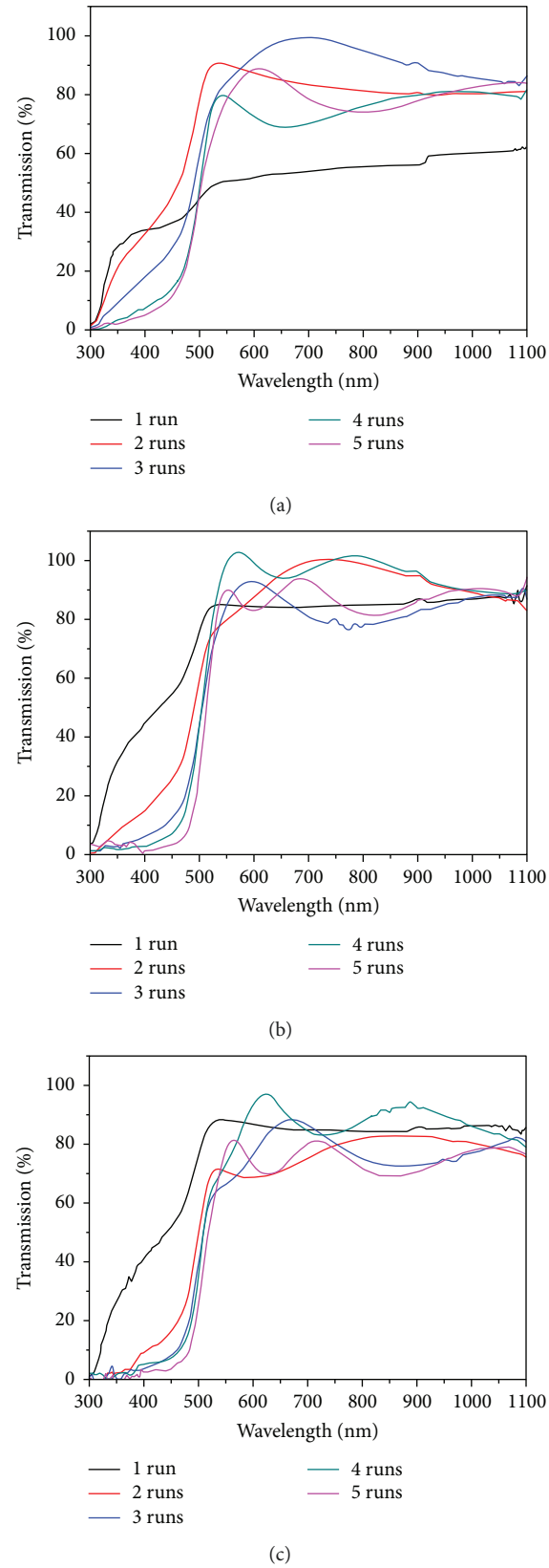

Figure 9: UV-Vis transmission spectra of CdS thin films synthesized at different number of runs and deposition times: (a) 1 min, (b) 5 min, and (c) 15 min.

Table 4: The band gap values in eV of the prepared CdS thin films as a function of the number of runs and deposition time.

CdS films	1 min	5 min	15 min
1 run	2.62	2.44	2.45
2 runs	2.49	2.43	2.44
3 runs	2.45	2.42	2.43
4 runs	2.43	2.42	2.42
5 runs	2.42	2.41	2.42

of runs is 1, 2, 3, 4, and 5 runs, respectively. (ii) The film thickness is slightly reduced when the time is varied from 5 to 15 min. This strange behavior is due to the solution supersaturation phenomenon which occurred at the colloidal precipitate state, where precipitated particles come to relatively pulverize the growing film.

Therefore, the results presented in Figure 6 are of great importance for the development of CdS films with a desired thickness without any supersaturation solution phenomenon. On the one hand, 5 min is recommended as the optimized deposition time. On the other hand, the number of runs can be varied to reach the desired thickness film.

The band gap values (E_g) of CdS thin films prepared at different numbers of runs and deposition times are reported in Table 4. A clear reduction of the band gap is noticed as the deposition time is increased up to 5 min for all numbers of runs. This observed change is likely attributed to (i) the increase in film thickness [43] (Figure 6) and/or (ii) the improvement of film crystallinity [36].

The absorbance spectra of the CdS thin films annealed at different temperatures are presented in Figure 10(a), while those of films prepared at different numbers of runs of 5 min are illustrated in Figure 10(b). No obvious difference is observed between the absorbance spectra of the as-deposited and the annealed films up to 400°C. Conversely, the film annealed at 550°C exhibits a drastic absorbance reduction between 300 and 450 nm, indicating a phase transition. On the other hand, Figure 10(b) indicates an increase in the absorbance intensity as the number of runs is increased. As revealed by the XRD results, this behavior is likely ascribed to the film crystallinity betterment.

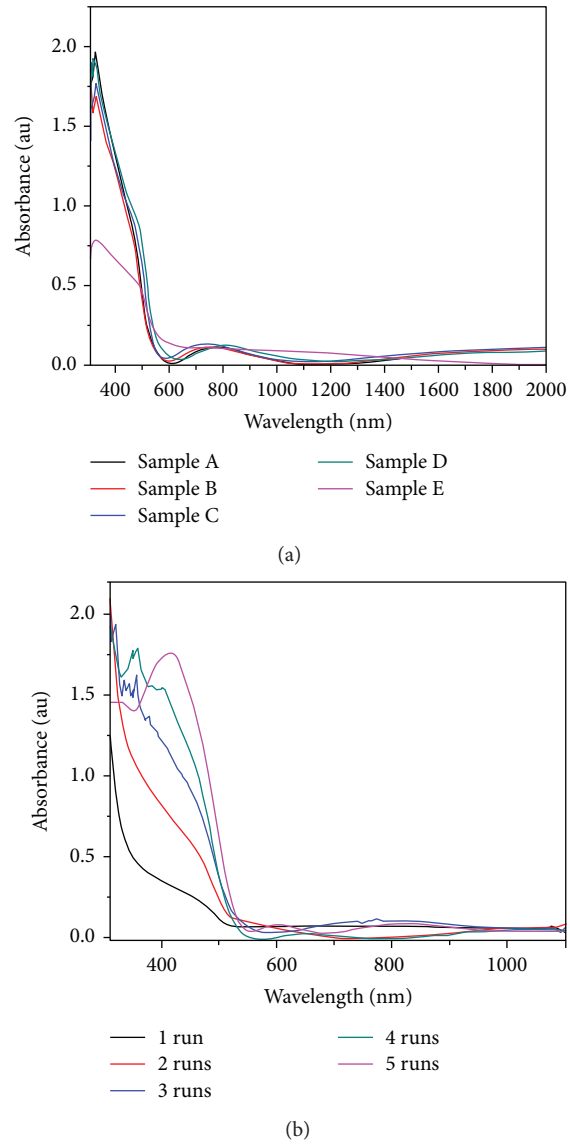

Figure 10: The absorbance spectra of (a) the as deposited and annealed films and (b) the films deposited in different numbers of runs.

4. Conclusion

CdS thin films, with good structural and morphological qualities, have been successfully synthesized using the CBD technique without any postannealing treatment. The band gap energy was found to be around 2.42 eV with 70 to 95% of optical transmittance in the visible range. The main finding of this work is to show experimentally that performing CBD deposition in "several runs of optimized time" allows avoiding the supersaturation solution phenomenon which constitutes the major problem uncounted when seeking to control the thickness of the deposited films. Therefore, by adopting this based CBD process, it is possible not only to overcome any film thickness limitation but also to grow the CdS films in a single technological step at a low solution temperature (60°C) as well. We believe that this technique paves the way to deposit thin layers on several flexible substrates requested in the embedded electronic field.

Data Availability

The data used to support the findings of this study are included within the article.

Disclosure

The research was carried out in the framework of a PhD thesis at Mohammed V University-Faculty of Science, in collaboration with the National Centre of Scientific and Technical Research (CNRST), Rabat, Morocco.

Conflicts of Interest

The authors declare that they have no conflicts of interest.

Acknowledgments

The authors wish to thank gratefully the National Center of Scientific and Technical Research (CNRST) and the staff of the UATRS Division, for the use of their equipment and technical assistance.

References

[1] L. Atourki, E. Vega, M. Mollar et al., "Impact of iodide substitution on the physical properties and stability of cesium lead halide perovskite thin films CsPbBr 3−x I x ($0 \le x \le 1$)," *Journal of Alloys and Compounds*, vol. 702, pp. 404–409, 2017.

[2] L. Atourki, E. H. Ihalane, H. Kirou et al., "Characterization of nanostructured ZnO grown by linear sweep voltammetry," *Solar Energy Materials & Solar Cells*, vol. 148, pp. 20–24, 2016.

[3] L. Atourki, E. Vega, B. Marí et al., "MAPbI 2.9-x Br x Cl 0.1 hybrid halide perovskites: shedding light on the effect of chloride and bromide ions on structural and photoluminescence properties," *Applied Surface Science*, vol. 390, pp. 744–750, 2016.

[4] M. Ouafi, B. Jaber, L. Atourki, R. Bekkari, and L. Laânab, "Improving UV stability of MAPbI3 perovskite thin films by bromide incorporation," *Journal of Alloys and Compounds*, vol. 746, pp. 391–398, 2018.

[5] B. Jaber and L. Laânab, "One step synthesis of ZnO nanoparticles in free organic medium: structural and optical characterizations," *Materials Science in Semiconductor Processing*, vol. 27, pp. 446–451, 2014.

[6] S. Yılmaz, S. B. Töreli, İ. Polat, M. A. Olgar, M. Tomakin, and E. Bacaksız, "Enhancement in the optical and electrical properties of CdS thin films through Ga and K co-doping," *Materials Science in Semiconductor Processing*, vol. 60, pp. 45–52, 2017.

[7] O. Vigil-Galán, F. A. Pulgarín, F. Cruz-Gandarilla et al., "Optimization of CBD-CdS physical properties for solar cell applications considering a MIS structure," *Materials and Design*, vol. 99, pp. 254–261, 2016.

[8] C. Chen, Y. Zhai, F. Li et al., "High efficiency CH 3 NH 3 PbI 3 :CdS perovskite solar cells with CuInS 2 as the hole transporting layer," *Journal of Power Sources*, vol. 341, pp. 396–403, 2017.

[9] M. A. Contreras, L. M. Mansfield, B. Egaas et al., "Wide bandgap Cu(In,Ga)Se2solar cells with improved energy conversion efficiency," *Progress in Photovoltaics: Research and Applications*, vol. 20, no. 7, pp. 843–850, 2012.

[10] National Renewable Energy Laboratory, "Efficiency_Chart," 2016, Http://Www.Nrel.Gov/Ncpv/Images/Efficiency_Chart.Jpg.

[11] M. Antoniadou, V. M. Daskalaki, N. Balis, D. I. Kondarides, C. Kordulis, and P. Lianos, "Photocatalysis and photoelectrocatalysis using (CdS-ZnS)/TiO2 combined photocatalysts," *Applied Catalysis B: Environmental*, vol. 107, no. 1-2, pp. 188–196, 2011.

[12] E. Sorokin, D. Klimentov, M. P. Frolov et al., "Continuous-wave broadly tunable high-power Cr: CdS laser," *Applied Physics B: Lasers and Optics*, vol. 117, no. 4, pp. 1009–1014, 2014.

[13] R. Bartlome, B. Strahm, Y. Sinquin, A. Feltrin, and C. Ballif, "Laser applications in thin-film photovoltaics," *Applied Physics B: Lasers and Optics*, vol. 100, no. 2, pp. 427–436, 2010.

[14] C. Bozkaplan, A. Tombak, M. F. Genişel, Y. S. Ocak, and K. Akkilic, "The influence of substrate temperature on RF sputtered CdS thin films and CdS/p-Si heterojunctions," *Materials Science in Semiconductor Processing*, vol. 58, pp. 34–38, 2017.

[15] M. Grün, A. Storzum, M. Hetterich et al., "Chlorine doping of cubic CdS and ZnS grown by compound source molecular-beam epitaxy," *Journal of Crystal Growth*, vol. 201-202, pp. 457–460, 1999.

[16] M. A. Islam, F. Haque, K. S. Rahman et al., "Effect of oxidation on structural, optical and electrical properties of CdS thin films grown by sputtering," *Optik - International Journal for Light and Electron Optics*, vol. 126, no. 21, pp. 3177–3180, 2015.

[17] S. Kar and S. Chaudhuri, "Shape selective growth of CdS one-dimensional nanostructures by a thermal evaporation process," *The Journal of Physical Chemistry B*, vol. 110, no. 10, pp. 4542–4547, 2006.

[18] S. Yilmaz, Y. Atasoy, M. Tomakin, and E. Bacaksiz, "Comparative studies of CdS, CdS:Al, CdS:Na and CdS:(Al-Na) thin films prepared by spray pyrolysis," *Superlattices and Microstructures*, vol. 88, pp. 299–307, 2015.

[19] D. Fernando, M. Khan, and Y. Vasquez, "Control of the crystalline phase and morphology of CdS deposited on microstructured surfaces by chemical bath deposition," *Materials Science in Semiconductor Processing*, vol. 30, pp. 174–180, 2015.

[20] T. Sainta Jostar., S. Devadason, and J. Suthagar, "Effect of CdS layers on opto-electrical properties of chemically prepared ZnS/CdS/TiO2 photoanodes," *Materials Science in Semiconductor Processing*, vol. 34, pp. 65–73, 2015.

[21] J. Maricheva, S. Bereznev, R. Naidu, N. Maticiuc, V. Mikli, and J. Kois, "Improved electrodeposition of CdS layers in presence of activating H2SeO3 microadditive," *Materials Science in Semiconductor Processing*, vol. 54, pp. 14–19, 2016.

[22] S. M. Pawar, B. S. Pawar, J. H. Kim, O.-S. Joo, and C. D. Lokhande, "Recent status of chemical bath deposited metal chalcogenide and metal oxide thin films," *Current Applied Physics*, vol. 11, no. 2, pp. 117–161, 2011.

[23] E. Çetinörgü, C. Gümüş, and R. Esen, "Effects of deposition time and temperature on the optical properties of air-annealed chemical bath deposited CdS films," *Thin Solid Films*, vol. 515, no. 4, pp. 1688–1693, 2006.

[24] B. Liu, R. Luo, B. Li et al., "Effects of deposition temperature and CdCl2 annealing on the CdS thin films prepared by pulsed laser deposition," *Journal of Alloys and Compounds*, vol. 654, pp. 333–339, 2016.

[25] F. Liu, Y. Lai, J. Liu et al., "Characterization of chemical bath deposited CdS thin films at different deposition temperature," *Journal of Alloys and Compounds*, vol. 493, no. 1-2, pp. 305–308, 2010.

[26] H. Zhang, X. Ma, and D. Yang, "Effects of complexing agent on CdS thin films prepared by chemical bath deposition," *Materials Letters*, vol. 58, no. 1-2, pp. 5–9, 2004.

[27] R. Zia, M. Riaz, Q. Ain, and S. Anjum, "Study the effect of thiourea concentration on optical and structural properties of CdS-nanocrystalline thin films prepared by CBD technique," *Optik - International Journal for Light and Electron Optics*, vol. 127, no. 13, pp. 5407–5412, 2016.

[28] K. Kaur, N. Kumar, and M. Kumar, "Strategic review of interface carrier recombination in earth abundant Cu–Zn–Sn – S–Se solar cells : current challenges and future prospects," *Journal of Materials Chemistry A*, vol. 5, no. 7, pp. 3069–3090, 2017.

[29] J. C. Ramos, I. Mejia, C. A. Martinez, and M. A. Quevedo-Lopez, "Direct on chip cadmium sulfide thin film transistors synthesized via modified chemical surface deposition," *Journal of Materials Chemistry C*, vol. 1, no. 40, p. 6653, 2013.

[30] A. Y. Jaber, S. N. Alamri, and M. S. Aida, "CdS thin films growth by ammonia free chemical bath deposition technique," *Thin Solid Films*, vol. 520, no. 9, pp. 3485–3489, 2012.

[31] M. B. Ortuño-López, M. Sotelo-Lerma, A. Mendoza-Galván, and R. Ramírez-Bon, "Chemically deposited CdS films in an ammonia-free cadmium-sodium citrate system," *Thin Solid Films*, vol. 457, no. 2, pp. 278–284, 2004.

[32] S. N. Sharma, R. K. Sharma, K. N. Sood, and S. Singh, "Structural and morphological studies of chemical bath-deposited nanocrystalline CdS films and its alloys," *Materials Chemistry and Physics*, vol. 93, no. 2-3, pp. 368–375, 2005.

[33] A. Khare, "Factors affecting the electro-optical and structural characteristics of nano crystalline Cu doped (Cd–Zn)S films," *Journal of Physics and Chemistry of Solids*, vol. 73, no. 7, pp. 839–845, 2012.

[34] J. Hiie, T. Dedova, V. Valdna, and K. Muska, "Comparative study of nano-structured CdS thin films prepared by CBD and spray pyrolysis: annealing effect," *Thin Solid Films*, vol. 511-512, pp. 443–447, 2006.

[35] B. Ghosh, B. K. Singh, P. Banerjee, and S. Das, "Nucleation and growth of CBD-CdS thin films on ultrathin aluminium layers and annealing induced doping," *Optik*, vol. 127, no. 10, pp. 4413–4417, 2016.

[36] M. Rami, E. Benamar, M. Fahoume, F. Chraibi, and A. Ennaoui, "Effect of the cadmium ion source on the structural and optical properties of chemical bath deposited CdS thin films," *Solid State Sciences*, vol. 1, no. 4, pp. 179–188, 1999.

[37] X.-Y. Peng, H.-W. Gu, T. Zhang, F. Qu, F.-Z. Ding, and H.-Y. Wang, "Morphological evolution of CdS films prepared by chemical bath deposition," *Rare Metals*, vol. 32, no. 4, pp. 380–389, 2013.

[38] L. Ma, X. Ai, and X. Wu, "Effect of substrate and Zn doping on the structural, optical and electrical properties of CdS thin films prepared by CBD method," *Journal of Alloys and Compounds*, vol. 691, pp. 399–406, 2017.

[39] S. B. Jambure, S. J. Patil, A. R. Deshpande, and C. D. Lokhande, "A comparative study of physico-chemical properties of CBD and SILAR grown ZnO thin films," *Materials Research Bulletin*, vol. 49, pp. 420–425, 2014.

[40] S. Tec-Yam, R. Patiño, and A. I. Oliva, "Chemical bath deposition of CdS films on different substrate orientations," *Current Applied Physics*, vol. 11, no. 3, pp. 914–920, 2011.

[41] M. A. Mahdi, Z. Hassan, S. S. Ng, J. J. Hassan, and S. K. M. Bakhori, "Structural and optical properties of nanocrystalline CdS thin films prepared using microwave-assisted chemical bath deposition," *Thin Solid Films*, vol. 520, no. 9, pp. 3477–3484, 2012.

[42] S. A. Zaki, M. I. Abd-Elrahman, A. A. Abu-Sehly, N. M. Shaalan, and M. M. Hafiz, "Thermal annealing of SnS thin film induced mixed tin sulfide oxides-Sn 2 S 3 for gas sensing: Optical and electrical properties," *Materials Science in Semiconductor Processing*, vol. 75, pp. 214–220, 2018.

[43] M. I. Abd-Elrahman, A. A. Abu-Sehly, Y. M. Bakier, and M. M. Hafiz, "Thickness and optical constants calculation for chalcogenide-alkali metal Se 80 Te 8 (NaCl) 12 thin film," *Spectrochimica Acta Part A*, vol. 184, pp. 243–248, 2017.

[44] A. E. Al-salami, A. Dahshan, and E. R. Shaaban, "Effect of film thickness on structural and optical properties of Cd-Zn-Te grown on glass and ITO substrates using electron beam evaporation," *Optik - International Journal for Light and Electron Optics*, vol. 150, pp. 34–47, 2017.

[45] M. Caglar, Y. Caglar, and S. Ilican, "The determination of the thickness and optical constants of the ZnO crystalline thin film by using envelope method," *Journal of Optoelectronics and Advanced Materials*, vol. 8, no. 4, pp. 1410–1413, 2006.

[46] J. K. Rajput, T. K. Pathak, V. Kumar, M. Kumar, and L. P. Purohit, "Annealing temperature dependent investigations on nano-cauliflower like structure of CdO thin film grown by sol–gel method," *Surfaces and Interfaces*, vol. 6, pp. 11–17, 2017.

[47] J. N. Ximello-Quiebras, G. Contreras-Puente, J. Aguilar-Hernandez, G. Santana-Rodriguez, and A. A. Readigos, "Physical properties of chemical bath deposited CdS thin films," *Solar Energy Materials and Solar Cells*, vol. 82, no. 1-2, pp. 263–268, 2004.

[48] R. Mariappan, M. Ragavendar, and V. Ponnuswamy, "Growth and characterization of chemical bath deposited Cd1−xZnxS thin films," *Journal of Alloys and Compounds*, vol. 509, no. 27, pp. 7337–7343, 2011.